REGIONAL TRAVEL-TIME PREDICTION, UNCERTAINTY, AND LOCATION IMPROVEMENT

Megan P. Flanagan and Stephen C. Myers

Lawrence Livermore National Laboratory

Sponsored by National Nuclear Security Administration
Office of Nonproliferation Research and Engineering
Office of Defense Nuclear Nonproliferation

Contract No. W-7405-ENG-48

ABSTRACT

We investigate our ability to improve regional travel-time prediction and seismic event location using an *a priori* three-dimensional (3D) velocity model of Western Eurasia and North Africa (WENA 1.0). Three principal results are presented. First, the 3D WENA 1.0 velocity model improves travel-time prediction over the IASPI91 model, as measured by variance reduction, for regional phases recorded at 22 stations throughout the modeled region, including aseismic areas. Second, a distance-dependent uncertainty model is developed and tested for the WENA 1.0 model. Third, relocation using WENA 1.0 and the associated uncertainty model provides an end-to-end validation test.

Model validation is based on a comparison of approximately 10,000 *Pg, Pn*, and *P* travel-time predictions and empirical observations from ground truth (GT) events. Ray coverage for the validation dataset provides representative, regional-distances sampling across Eurasia and North Africa. The WENA 1.0 model markedly improves travel-time predictions for most stations with an average variance reduction of 14% for all ray paths. We find that improvement is station dependent, with some stations benefiting greatly from WENA predictions (25% at OBN and 16% at BKR), some stations showing moderate improvement (12% at ARU and 17% at NIL), and some stations benefiting only slightly (7% at AAE and 8% at TOL). We further test WENA 1.0 by relocating five calibration events. Again, relocation of these events is dependent on ray paths that evenly sample WENA 1.0 and therefore provide an unbiased assessment of location performance. These results highlight the importance of accurate GT datasets in assessing regional travel-time models and demonstrate that an *a priori* 3D model can markedly improve our ability to locate small magnitude events in a regional monitoring context.

OBJECTIVE

Our objective is to improve the accuracy of seismic location estimates and to reduce the uncertainty of the estimated locations. As we focus on the geographic region of western Eurasia, the Middle East, and north Africa, we develop, test, and validate 3D model-based travel-time prediction models for about 30 stations in the study region. Improvement in travel-time prediction is quantified, and final calibrations are tested in an end-to-end relocation of five events with known location accuracy between 1 km and 5 km. Improvement in both location and uncertainty estimates are assessed.

RESEARCH ACCOMPLISHED

WENA1.0: 3D *a priori* Geophysical Model

We demonstrate improvement in travel-time prediction of P-waves and regional location performance using the WENA1.0 model (Figure 1) (Pasyanos, et al., 2004). WENA1.0 is a 3D Earth model of the crust and upper mantle that is made up of geophysically distinct regions. Each regional velocity model is determined using previous a geophysical studies and analogy with similar geologic provinces. Because the regional models are developed independently, the WENA1.0 is an *a priori* model that is not based on any one data set. Because the model is developed using geophysical analogy, it is particularly applicable to aseismic regions where calibration data are sparse. The model resolution is 1° by 1°, and the data are primarily compiled from the Exxon Map, Crust 5.1 (Mooney et al., 1998), topography, seismicity, phase blockages, *Pn* tomography, surface-waves, receiver functions, a sediment map from Laske and Masters (1997), crustal regionalizations by Bhattacharyya et al. (2000) and Walter et al. (2000), and the mantle model 3SAC by Nataf and Ricard (1996).

The WENA1.0 model has been extensively evaluated using a number of data sets, including surface wave dispersion measurements, teleseismic receiver functions, gravity, and waveform analysis (Pasyanos et al., 2004). In this study we test the improvement of P-wave travel-time prediction and location performance using a newly developed validation data set.

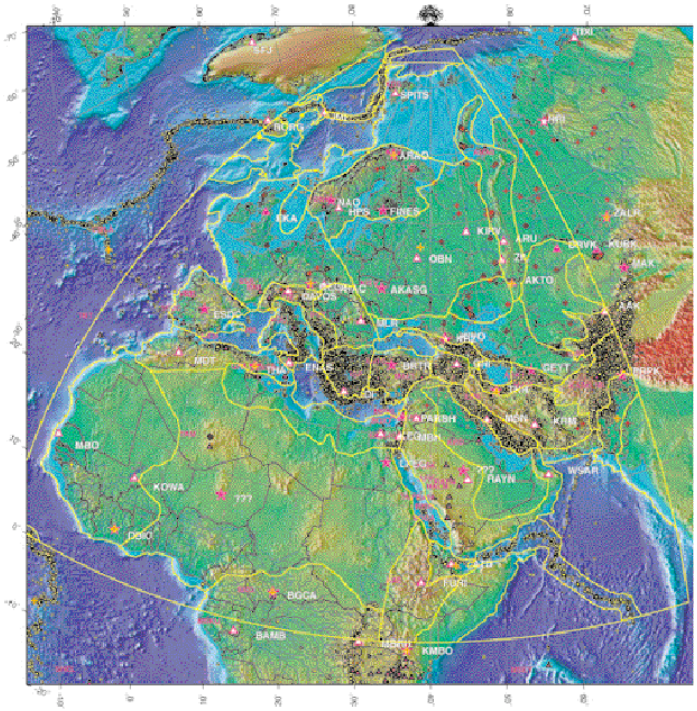

Figure 1. Crustal regionalization used in the WENA1.0 geophysical model. There are about 45 base models, outlined in yellow, which describe *P*- and *S*-wave velocities, attenuation, and density (Pasyanos et al., 2004).

Validation Data Set

We validate improvement in travel-time prediction using well-recorded events with accurate locations. Each validation event meets the network-coverage accuracy criteria of Bondar et al. (2004) or the location accuracy constrained by nonseismic means (e.g., explosions with know sources). Epicenter accuracy ranges from perfect (for known locations) to 25 km for events constrained with a teleseismic network. A procedure similar to the leave-one-out validation described in (Myers and Schulz, 2000) is used to check the consistency of each arrival-time observation. This procedure is a considerable improvement over outlier removal based on statistics of the whole population, because local trends and biases are taken into consideration. Culling based on location accuracy and arrival-time consistency produces a self-consistent data set of accurate travel-time measurements. Ray paths for the validation data set are shown in Figure 2. Raypath coverage is excellent over much of the region, and our new data set provides considerable improvement in ray coverage for aseismic regions, such as North Africa.

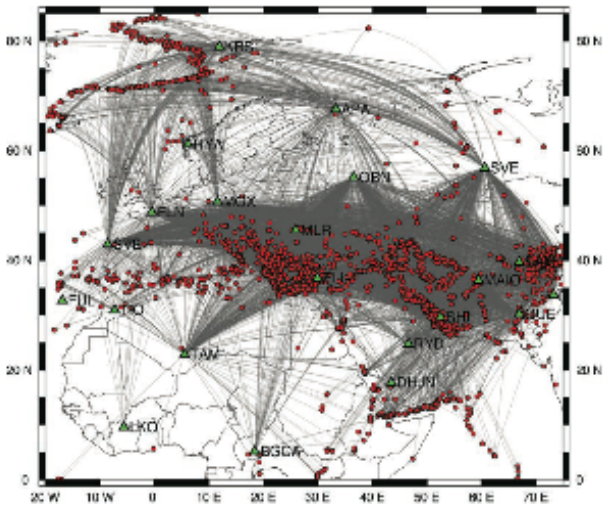

Figure 2. Map of raypath coverage for WENA region. Paths are from the GT events to 23 stations and show good coverage of the entire model region.

Our ultimate goal is to improve regional-network location accuracy. We test location performance by relocating five events with an epicenter accuracy of 5 km or better (Figure 3). Four of the events meet the local-network-coverage criteria of Bondar et al., (2004) for a 5 km epicenter accuracy at 95% confidence. One event is taken from the catalog of Soviet peaceful nuclear explosions (PNEs) reported in Sultanov et al., (1999). The PNE event is reported to have an accuracy of 1 km. These five events are well distributed geographically, and they are recorded at more regional-distance stations than other events with similar location accuracy. Therefore, the validation events provide even ray sampling over the model and an unbiased assessment of travel-time prediction accuracy and location performance.

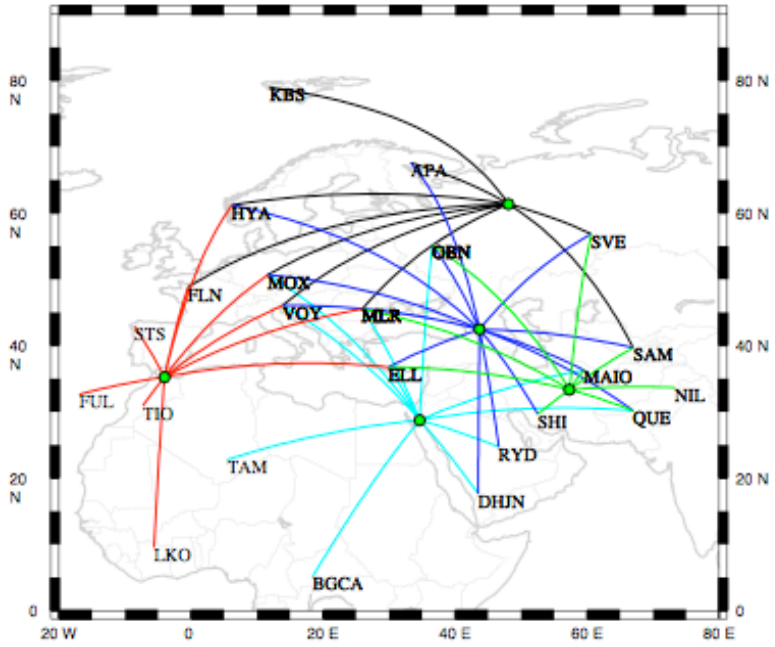

Figure 3. Five reference events used to test location accuracy and the 23-station network used for relocation.

3D Finite Difference Travel-time Calculations

We use the finite-difference method (FD) of Vidale (1988) with modifications by Hole and Zelt (1995) to compute travel times through the WENA1.0 velocity model. This technique propagates wave fronts radially outward from a point source using each grid (or time) point as a secondary source for each successive grid point. This procedure is more efficient and accurate than ray tracing because it is able to treat sharp velocity gradients that produce refracted, diffracted, or head waves in addition to direct phases. Furthermore, by taking advantage of travel-time reciprocity, we place the ray-tracing source at the station locations and calculate travel times to a 3D are estimated through interpolation of the travel-time prediction grid.

We have made two significant modifications to the finite difference code. First, we adapt it to read in 3D velocity models instead of 1D, enabling it to compute times through our WENA1.0 (or any custom 3D) model. Second, we apply a Cartesian-to-spherical coordinate transformation to the source and receiver locations that are input to the code (Flanagan et al., 2004). Therefore, instead of using an earth-flattening approach (which may not be applicable to 3D models), we literally create a spherical grid of points. This modification allows us to compute travel-times out to regional and near-teleseismic distances (~13° to 30°). The code is run in a volume of dimensions of roughly 35° by 50° laterally and 1,200 to 1,500 km deep with a grid spacing of 5 km. The grid spacing is determined empirically as a tradeoff between the accuracy of the travel-time prediction and computer memory limitations, and we find that a grid spacing of 5 km provides a reasonable accuracy (i.e., timing errors of approximately 0.25 s, see Figure 3).

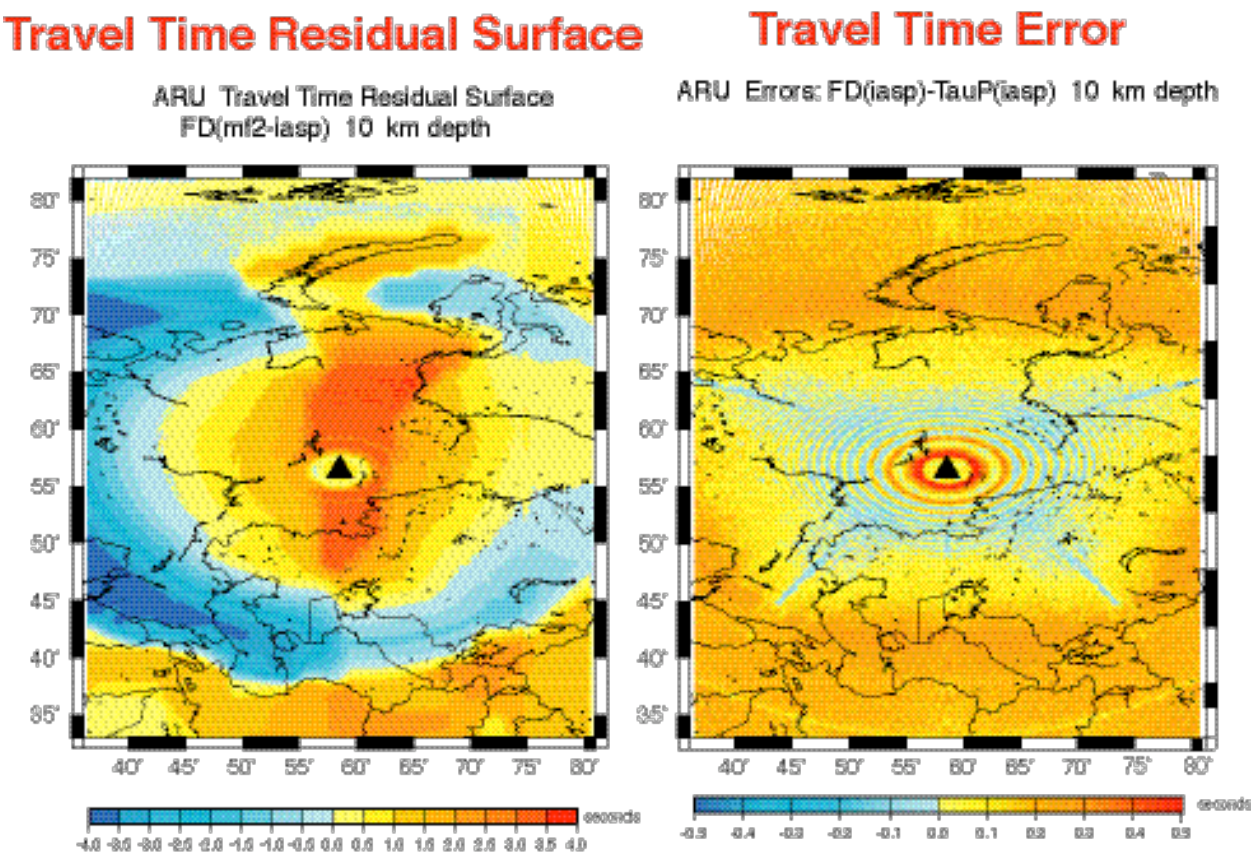

Figure 4. a) Travel-time residual surface for station ARU (black triangle); this surface shows the variations in travel-time as a result of 3D structure in the WENA1.0 model relative to the 1D IASP91 model. (b) Numerical errors in the FD code are quantified by subtracting theoretical 1D *IASP91* times computes from *TauP* (Crotwell, et al., 1999) from the IASP91 times predicted by the 3D, FD computation. Blue indicates fast regions, and red indicates slow; note the difference in the scale.

Result 1: Improvement in Travel-time Prediction

We compute 3D travel-time prediction models for first arriving *P*-wave travel-times predicted by the FD algorithm. The total predicted arrival time is computed along a regular grid in latitude, longitude grid with 25 km sampling. Depth is regularly sampled at intervals of 10 km down to 50 km. Each prediction model provides station-specific travel-times for regional to near-teleseismic distances, which can be used to locate regional-distance events. The difference between WENA1.0 and IASP91 travel-time predictions at four stations are shown in Figure 5. The example in Figure 5 is for a source depth of 10 km. We find travel-time differences of up to 6 seconds relative to IASP91. Extreme differences in travel-time prediction are generally caused by anomalous upper-mantle velocity, thick crust, and/or thick sediments. Note that the patterns in these correction surfaces correlate with the structural features in the WENA1.0 model; fast predictions are seen to the north (e.g., Russian platform) but slow anomalies are seen in the south (e.g. Turkey, Mediterranean, Iran).

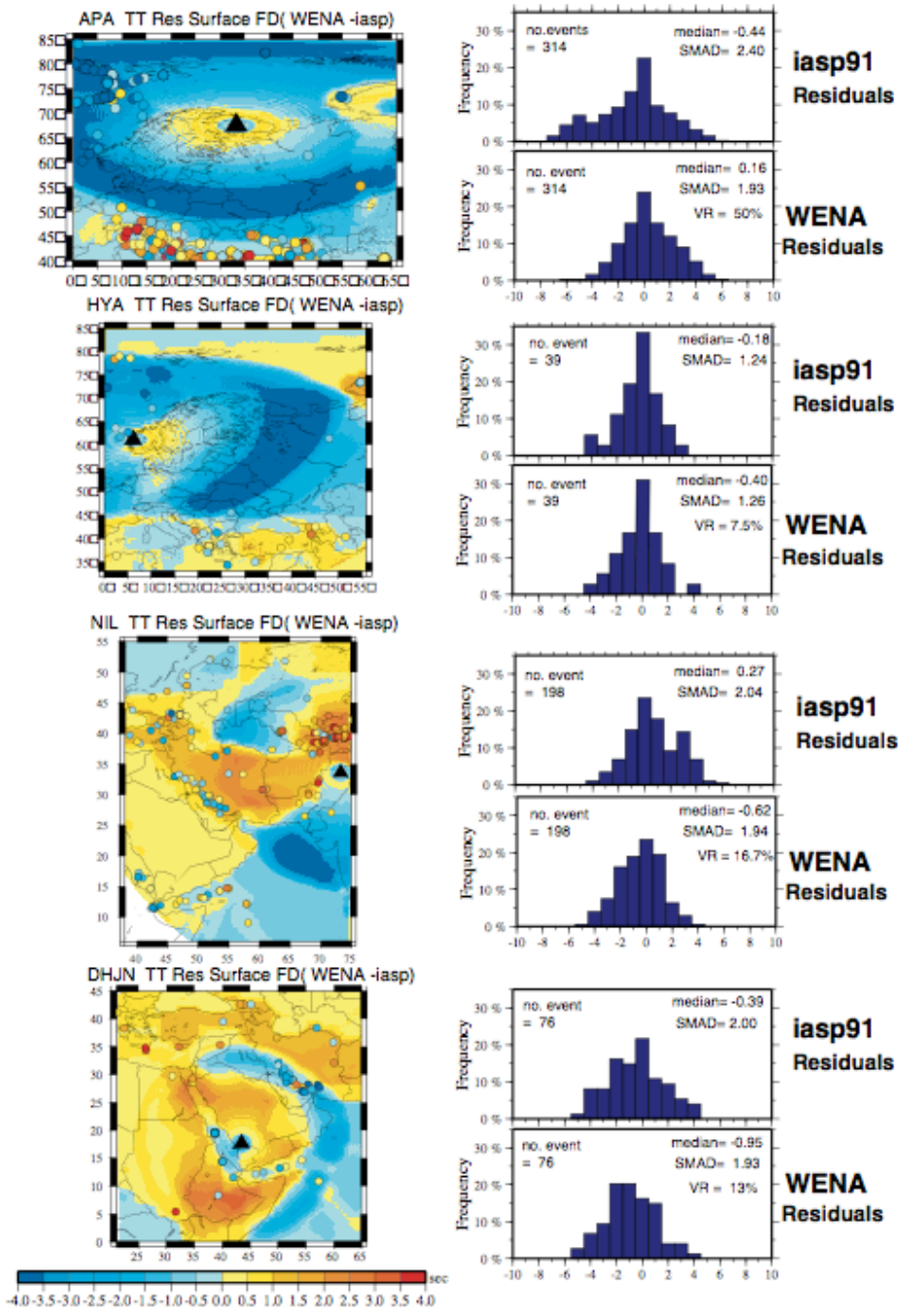

Figure 5. (left) Travel-time residual surfaces at 10 km depth; these model-based correction surfaces are computed by subtracting the IASP91 predicted time from the WENA1.0 predicted time. Blue indicates fast regions, and red indicates slow. The (GT-IASP91) residuals are plotted on top of the correction surfaces. (right) Histograms of GT-IASP91 and GT-WENA1.0 residuals showing the variance reduction for observed times at different stations. While WENA1.0 does not improve travel-time prediction in all cases, we find that overall prediction is improved by 15% to 20%.

Variation in residual variance is generally on the order of 15% to 20% for the stations we tested (e.g., Station NIL in Figure 5). The performance at any given station is quite variable, however, with improvement ranging from 50% (e.g. Station APA in Figure 5) to negligible.

Result 2: Uncertainty Model for WENA1.0

Travel-time prediction uncertainty is commonly distance dependent. Distance dependent uncertainty results from velocity-model errors that cause cumulatively more bias in travel-time prediction with distance. In this study we fit a distance-dependent uncertainty model using our validation data set. The simple fitting procedure entails calculating the mean and spread of the residual distribution in distance bins. Statistics of each bin are then used to determine the uncertainty at a given confidence in each distance bin. The distance-dependent uncertainty for WENA is shown in Figure 6. Because the uncertainty model is based on a data set that covers nearly all of the WENA model, it is applicable over the whole model.

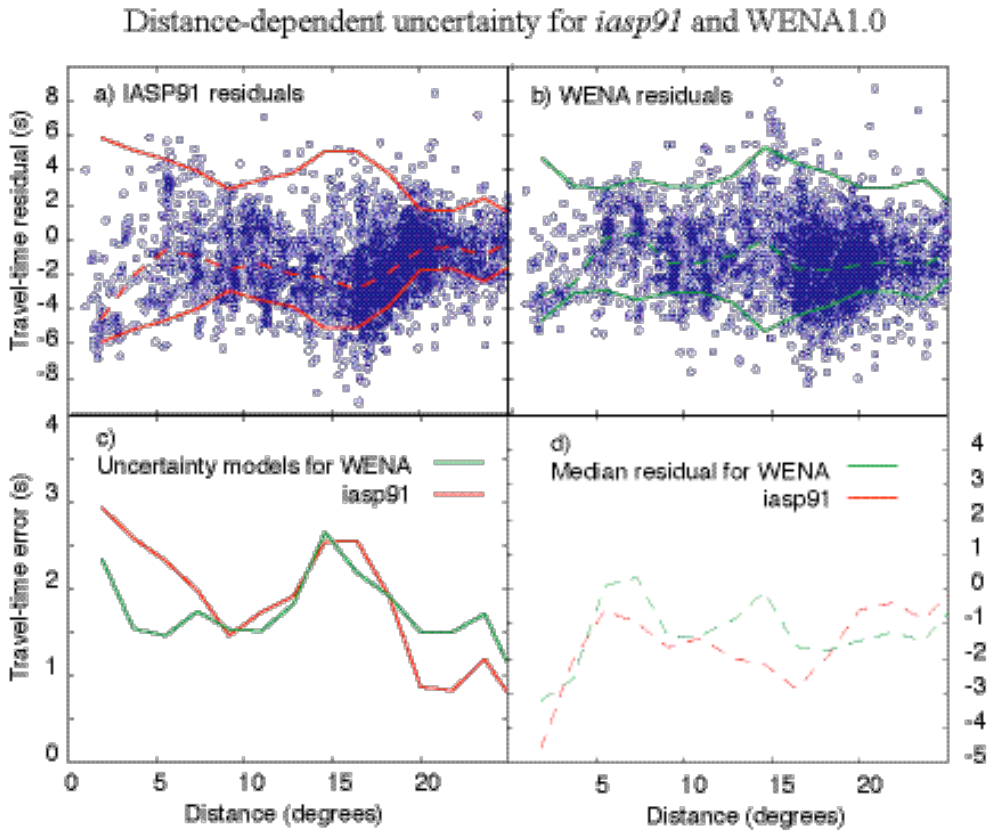

Figure 6. Distance-dependent uncertainty for IASP91 and WENA1.0. Note the nonstationarity and correlation in travel-time uncertainty between 1,000 and 2,800 km; uncertainty increases and errors are correlated (negative bias).

We use variogram modeling to assess the spatial statistic of the travel-time residuals. This approach examines the difference between residuals as a function of inter-event distance. An example of variogram analysis is shown in Figure 7. Note that the variograms do not approach zero for points that are nearly colocated (i.e., data are not perfectly correlated) because of errors associated with determining travel-time residuals. However, it is apparent that the variograms reach minima (correlation is maximum) for points close together, and the variograms increase (correlation decreases) as points become separated by greater distance. The 3D WENA1.0 model accomplishes two goals: improving the travel-time prediction by reducing the overall variance of residuals and reducing the nonstationarity of the uncertainties.

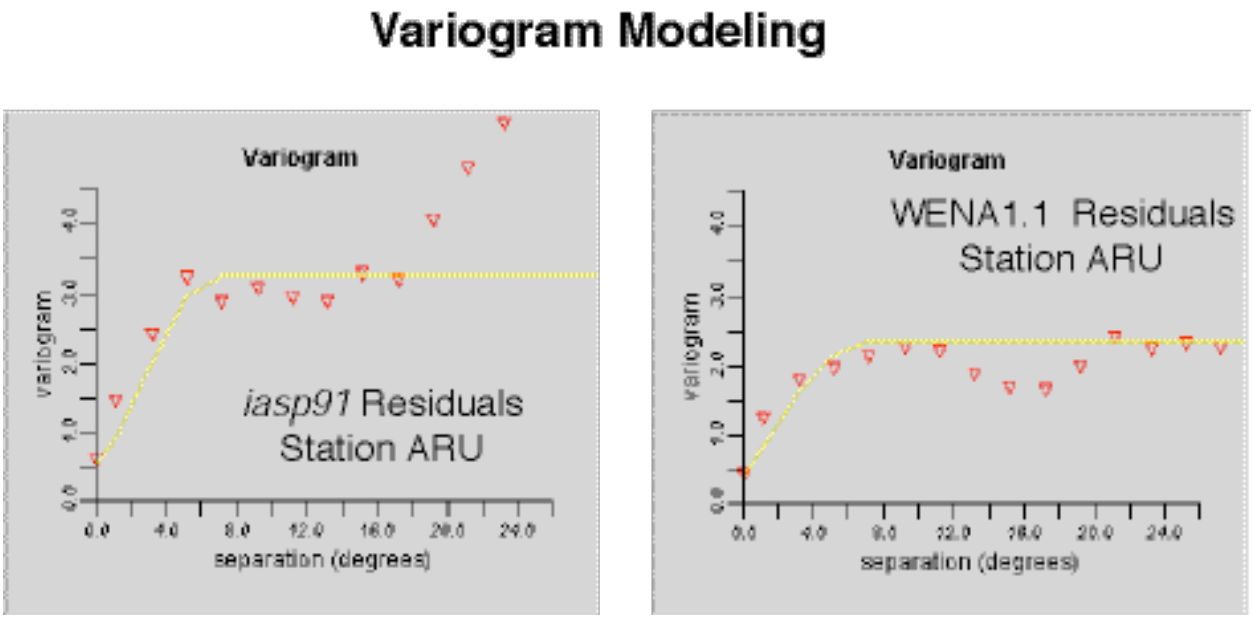

Figure 7. Variograms of travel-time residuals at station ARU for both the WENA1.0 and IASP91 velocity models. Crosses are the data variogram values in 1.0 degree bins; solid lines are the model variograms determined by curve fitting. The sill is the background variance of the data, the range is the distance at which correlation between points is zero, and the nugget is the covariance of colocated points. The IASP91 variogram is nonstationary (levels off at the sill, then increases again). The nonstationarity is caused by long-period features in the residual structure. WENA1.0 improves prediction of long-period residual features, and the variogram is relatively flat after the sill is reached.

Result 3: Improvement in Location using WENA1.0

Test events for location improvement are shown in Figure 3. Each of these events was relocated using first-arriving P-waves and either the IASP91 or WENA1.0 model. Figure 8 shows the result of these relocation tests. Average IASP91 mislocation is 19 km. WENA1.0 improves location accuracy by an average of 6.8 km to 12.2 km. This degree of improvement is similar to other calibration efforts that make use of tomographic models and GT15 calibration events.

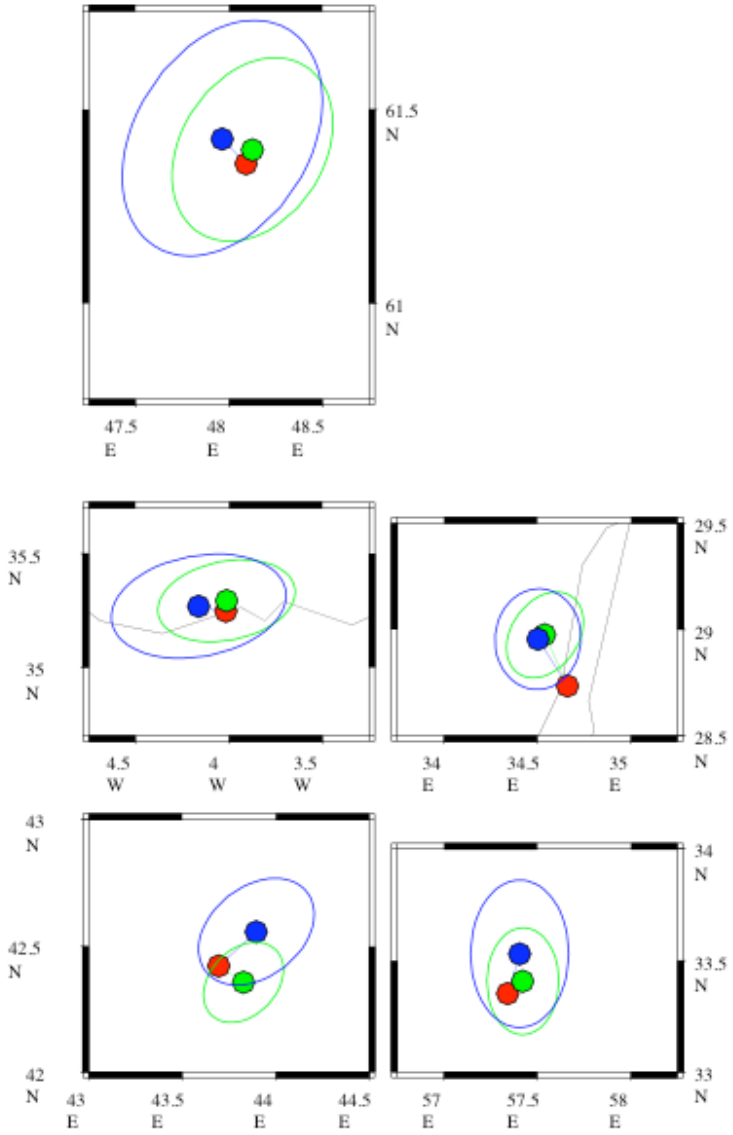

Figure 8. Results of location tests for WENA1.0 (green) and IASP91 (blue). Ground truth locations are shown in red.

The travel-time uncertainty model shown in Figure 6 is used to estimate coverage ellipses shown in Figure 8. In each instance, the coverage ellipse is smaller for the WENA1.0 model than the IASP91 model. This is consistent with our finding that WENA1.0 improves location accuracy. In most instances, the known location lies within the 95% confidence ellipse, suggesting that our error model is representative, but the known location is outside the 95% coverage ellipse in one instance. The one instance is likely to be a statistical anomaly, but further investigation is warranted.

CONCLUSIONS AND RECOMMENDATIONS

We test the applicability of the WENA1.0 model for regional seismic location. Tests include travel-time prediction performance for a large validation data set, and improvements in location accuracy for a limited, geographically distributed set of validation events. Three main findings are as follows:

- Application of WENA1.0 improves travel-time prediction by approximately 20% on average. For some stations, improvement approaches 50%, and for other stations improvement is negligible.
- Test of location improvement suggest that WENA1.0 improves epicenter accuracy in most cases, and uncertainty estimates are representative of observed mislocation.
- Improvement in WENA1.0 travel-time predictions primarily stems from the removal of long wavelength anomalies in the IASP91 predictions. These long wavelength features cause undesirable correlations in travel-time predictions that violate assumptions of most location algorithms.

REFERENCES

Bhattacharyya, J., W. Walter, M. Flanagan, J. O'Boyle and M. Pasyanos (2000), Preliminary definition of geophysical regions in Western Eurasia, UCRL-ID-138402, LLNL (http://www.llnl.gov/tid/lof/documents/pdf/237980.pdf).

Bondar, I., S.C. Myers, E. R. Engdahl and E.A. Bergman, (2004) Epicenter accuracy based on seismic network criteria, *Geophys. J. Int*, 156, 483-496, 2004.

Crotwell, H.P., T.J. Owens, and J. Ritsema (1999), The TauP ToolKit: Flexible seismic travel-time and raypath utilities, *Seism. Res. Lett.*, 70, 154-160.

Flanagan, M. P., S. C. Myers, K. D. Koper, (2004), Regional travel-time uncertainty and seismic event location improvement using 3-Dimensional *a priori* velocity models, *in preparation.*

Hole, J.A. and B.C. Zelt, (1995), 3-D Finite Difference Reflection Travel Times, *Geophys. J. Int.,* 121, 427-434.

Kennett, B.L.N. and E.R. Engdahl, (1991), Traveltimes for global Earthquake reference location and phase identification, *Geophys. J. Int, 105*, 429-465.

Laske, G. and T.G. Masters (1997), A global digital map of sediment thickness, EOS Trans. AGU, 78, F483.

Mooney, W.D., G. Laske and G. Masters, (1998) CRUST 5.1: A global crustal model at 5°x5°. *J. Geophys. Res.*, 103, 727-747, 1998.

Myers, S.C. and C.A. Schultz, (2000), Improving Sparse Network Seismic Location with Bayesian Kriging and Teleseismically Constrained Calibration Events, *Bull. Seism. Soc. Am.,* 90, 199-211

Nataf, H.C., and Y. Ricard (1996), 3SMAC: an a priori tomographic model of the upper mantle based on geophysical modeling, Physics of the Earth and Planetary Interiors, 95, 101-122.

Pasyanos, M. E., W. R. Walter, M. P. Flanagan, P. Goldstein and J. Bhattacharyya (2004), Building and testing an a priori geophysical model for western Eurasia and North Africa, Pure and Applied Geophysics, 161, 235-281.

Schultz, C. A, and S. C. Myers, (1998), Nonstationary Bayesian Kriging: A predictive technique to generate spatial corrections for seismic detection, location, and identification, *Bull. Seism. Soc. Am.*, 88, 1275-1288.

Sultanov, D.D., J.R. Murphy, and K.D. Rubinstein, A seismic source summary for Soviet peaceful nuclear explosions, Bull. Seismol. Soc. Am., 89, 640-647, 1999.

Vidale, J., (1988) Finite-difference Calculation of Travel Times, *Bull. Seismol. Soc. Am.,* 78, 2062-2076.

Walter, W.R., M.E. Pasyanos, J. Bhattacharyya and J. O'Boyle (2000), MENA 1.1 - An updated geophysical regionalization of the Middle East and North Africa, UCRL-ID-138079, LLNL (http://www.llnl.gov/tid/lof/documents/pdf/237521.pdf).